Accepted Manuscript

Preparation, characterization and in vitro antioxidant and cytotoxicity studies of some 2,4-dichloro-N-[di(alkyl/aryl)carbamothioyl]benzamide derivatives

Nanjappan Gunasekaran , Vellingiri Vadivel , Nathan R. Halcovitch , Edward R.T. Tiekink

PII: S2405-8300(16)30065-9
DOI: 10.1016/j.cdc.2016.11.007
Reference: CDC 33

To appear in: *Chemical Data Collections*

Received date: 22 August 2016
Revised date: 11 November 2016
Accepted date: 20 November 2016

Please cite this article as: Nanjappan Gunasekaran , Vellingiri Vadivel , Nathan R. Halcovitch , Edward R.T. Tiekink , Preparation, characterization and in vitro antioxidant and cytotoxicity studies of some 2,4-dichloro-N-[di(alkyl/aryl)carbamothioyl]benzamide derivatives, *Chemical Data Collections* (2016), doi: 10.1016/j.cdc.2016.11.007

Graphical abstract

Acylthiourea derivatives were prepared and characterized by analytical and spectral methods. Three dimensional structures of all three compounds were derived by single crystal X-ray crystallography. The acylthiourea derivatives were subjected to *in vitro* antioxidant and cytotoxicity studies and all the synthesized compounds show good anti-oxidant and cytotoxic potential.

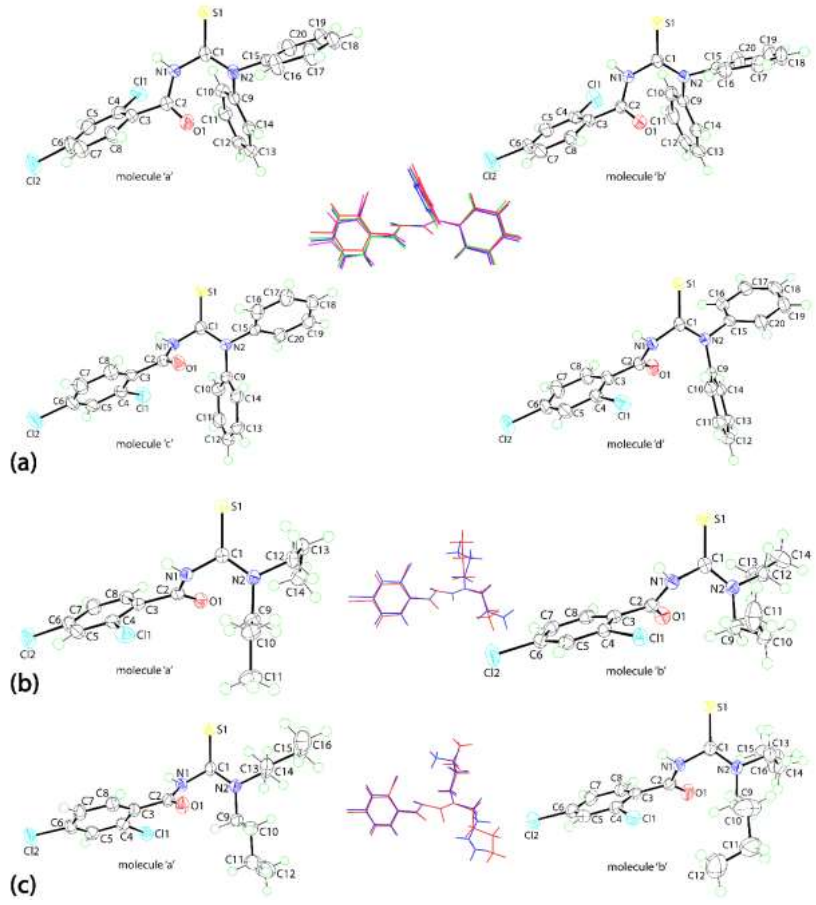

Preparation, characterization and *in vitro* antioxidant and cytotoxicity studies of some 2,4-dichloro-*N*-[di(alkyl/aryl)carbamothioyl]benzamide derivatives

Nanjappan Gunasekaran [a,*], Vellingiri Vadivel [b], Nathan R. Halcovitch [c], Edward R.T. Tiekink [d]

[a] *Centre for Nanotechnology & Advanced Biomaterials (CeNTAB), SASTRA University, Thanjavur 613 401, India*

[b] *Centre for Advanced Research in Indian System of Medicine (CARISM), SASTRA University, Thanjavur 613 401, India*

[c] *Department of Chemistry, Lancaster University, Lancaster LA1 4YB, United Kingdom*

[d] *Research Centre for Crystalline Materials, Faculty of Science and Technology, Sunway University, 47500 Bandar Sunway, Selangor Darul Ehsan, Malaysia*

ABSTRACT

In the present study, three biologically active, substituted acyl thiourea compounds (**1**–**3**) have been synthesized from 2,4-dichlorobenzoyl chloride, potassium thiocyanate and the corresponding secondary amine in dry acetone. As analytical and spectral data of **1** and **3** have already been discussed in the literature, only the compound **2** was characterized by elemental analyses, UV–Visible, FT–IR, ^{1}H & ^{13}C NMR spectroscopic techniques. The molecular structures of **1**–**3** were determined by single crystal X-ray crystallography which shows twists of up to 70º about the (S=)**C**–**N**C(=O) bonds. All the synthesized compounds show good antioxidant property and cytotoxic potential against Ehrlich Ascites Carcinoma (EAC) cancer cell line.

Keywords: Thiourea derivatives, X-ray crystallography, Antioxidant activity, Cytotoxicity, EAC cell line

* Corresponding author. Tel.: +914362304346; fax: +91 4362 264120.

E-mail address: sciguna@scbt.sastra.edu (N. Gunasekaran).

Specifications Table

Subject area	Organic Chemistry, X-ray Crystallography
Compound	2,4-dichloro-*N*-[di(alkyl/aryl)carbamothioyl]benzamide derivatives
Data category	Elemental analyses, UV–Visible, FT–IR, ^{1}H & ^{13}C NMR spectroscopy and X-ray Crystallography data
Data acquisition format	CIF for crystallography
Data type	Analyzed
Procedure	Acylthiourea compounds were synthesized from 2,4-dichlorobenzoyl chloride, potassium thiocyanate and the corresponding secondary amine in dry acetone. Single crystals of synthesized compound for X-ray diffraction studies were grown at room temperature from their respective dichloromethane solutions.
Data accessibility	CCDC 1493453-1493455, URL:https://summary.ccdc.cam.ac.uk/structure-summary-form

1. Rationale

The significance of acylthiourea derivatives has been investigated for over a century and has given rise to diverse applications in various fields. Thiourea derivatives have widely been used in analytical and process chemistry applications [1]. For the liquid–liquid extraction and pre-concentration of platinum group metals, *N*,*N*-dialkyl-*N*′-acylthioureas were used as ionophores [2]. Transition-metal complexes comprising *N*,*N*-dialkyl-*N*′-acylthiourea ligands acted as effective catalysts in oxidation catalysis [3-6]. Many corrosion studies confirmed the corrosion prevention ability of acylthioureas on the surface of a wide range of metals in different corrosive environments [7–9]. Acylthioureas are convenient synthons for the preparation of versatile heterocyclic compounds through cyclization [10,11]. Particularly relevant to the present investigation is that thiourea derivatives are well known for their biological activities such as antimicrobial [12,13], antifungal [14], antibacterial [15], insecticidal [16], herbicidal activity [17], etc. Polysubstituted acylthiourea and its fused heterocycle derivatives were utilized as inhibitors of influenza virus [18]. In addition, acylthiourea derivatives and their coordination

compounds exhibit strong antitumor and anticancer activity [19]. Benzoylphenylthiourea derivatives possess potent antitumor activity against both pancreatic and prostate cancer cell lines [20]. Thiourea derivatives bearing benzothiazole moiety have been used as powerful anticancer agents [21]. We report herein synthesis and X-ray crystallographic studies of three new derivatives, namely 2,4-dichloro-*N*-(diphenylcarbamothioyl)benzamide (**1**), 2,4-dichloro-*N*-(dipropylcarbamothioyl)benzamide (**2**) and 2,4-dichloro-*N*-(dibutylcarbamothioyl)benzamide (**3**) and their *in vitro* antioxidant and cytotoxicity against EAC cancer cell line.

2. Procedure

2.1. Materials and methods

All chemicals used in this work were procured from commercial sources and utilized without further purification. The organic solvents were distilled and purified according to literature procedures. Elemental analyses were performed by a Vario EL AMX-400 elemental analyzer. Uncorrected melting points were obtained in open capillary tubes on a Sigma melting point apparatus. FT–IR spectra in the mid–IR region (4000–600 cm^{-1}) were recorded on a NicoletiS5 FT–IR spectrophotometer with KBr pellets. UV–vis spectra in the range 800 to 200 nm were recorded in ethanol solutions using a PG Instruments double-beam UV–vis spectrophotometer (Model T90+) with a quartz cell of 1 cm path length. ^{1}H and ^{13}C NMR spectra were recorded on BrukerAvance 400 MHz instrument in DMSO-d_6 with TMS as an internal standard.

2.2. Synthesis

A solution of 2,4-dichlorobenzoyl chloride (1.0473 g, 5mmol) in acetone (50 mL) was added drop wise to a suspension of potassium thiocyanate (0.4859 g, 5 mmol) in anhydrous acetone (50 mL). The reaction mixture was heated under reflux for 45 minutes and then cooled

to room temperature. A solution of diphenyl amine / di-n-propyl amine / di-n-butyl amine (0.5059–0.8461 g, 5 mmol) in acetone (30 mL) was added and the resulting mixture was stirred for 2 h at room temperature. Hydrochloric acid (0.1 N, 500 mL) was added and the resulting white solid was filtered off, washed with water and dried *in vacuo* [22]. Single crystals of **1**-**3** for X-ray diffraction studies were grown at room temperature from their respective dichloromethane solutions. As analytical and spectral data of **1** and **3** have already been discussed in the literature [22], elemental analyses, UV–Visible, FT–IR, ^{1}H & ^{13}C NMR spectroscopic data are given only for compound **2**.

*Synthesis of 2,4-dichloro-N-(dipropylcarbamothioyl)benzamide (**2**)*

Yield: 85%. White solid. m.p. 153 ^{o}C. Anal. Calc. for $C_{14}H_{18}Cl_2N_2OS$ (%): C, 50.45; H, 5.44; N, 8.41; S, 9.62. Found: C, 50.41; H, 5.42; N, 8.37; S, 9.58. UV [Ethanol, λ in nm (ε in $dm^3mol^{-1}cm^{-1}$)]: 207 (30,240), 286 (8,522). FT–IR (KBr): ν = 3230 (N–H), 1661 (C=O), 1210 (C=S) cm^{-1}. ^{1}H NMR (DMSO-d_6): δ 10.90 (s, 1H, N–H), 7.46–7.69 (m, 3H, aromatic), 3.85 (t, *J* = 8 Hz, 2H, CH_2), 3.54 (t, *J* = 8 Hz, 2H, CH_2), 1.65–1.75 (m, 4H, CH_2), 0.85 (t, *J* = 8 Hz, 3H, CH_3), 0.92 (t, *J* = 8 Hz, 3H, CH_3) ppm. ^{13}C NMR (DMSO-d_6): δ 179.8 (C=S), 163.2 (C=O), 127.8, 129.7, 130.7, 131.8, 134.8, 135.6 (aromatic), 54.2, 54.6 (CH_2), 19.5, 21.7 (CH_2), 11.4, 11.5 (CH_3) ppm.

2.3. X-ray crystallography

Intensity data for **1**–**3** were measured at 100 K on a dual-source Rigaku Oxford Diffraction diffractometer with a CCD detector using CuKα radiation, λ = 1.54184Å [23]. The structures were solved by direct methods (SHELXS97 [24] through the WinGX Interface [25]) and refined (anisotropic displacement parameters, C-bound H atoms in the riding model approximation and a weighting scheme of the form $w = 1/[\sigma^2(F_o^2) + aP^2 + bP]$ where $P = (F_o^2 +$

$2F_c^2$)/3) with SHELXL2014/7 on F^2 [26]. The N-bound hydrogen atoms were located from difference maps and refined with N–H = 0.88±0.01 Å. In the refinement of **1**, the chloride atom at the C4 position of molecule 'a' was disordered over the C4/C8 positions. The major component had a site occupancy factor = 0.850(3). The analyzed sample was a two-component twin [twin law: -1 0 0, 0 -1 0, 0.721 0 1] and the minor component fraction was 0.3905(6). In the final refinement, 14 reflections with poor agreement were omitted. In the refinement of **3**, both molecules exhibited disorder in the C4-bound chloride atoms. The major components had site occupancy factors = 0.8667(17) and 0.9379(18) for molecules 'a' and 'b', respectively. One of the n-butyl groups was also found to be disordered so that the C14 and C15 atoms were located over two positions; major component = 0.740(6). The molecular structure diagrams shown in Fig. 1 were drawn with 70% displacement ellipsoids [25], and overlay diagrams, also in Fig. 1, were drawn in QMol [27]. Crystallographic data are collated in Table 1. The crystal packing diagrams were generated with DIAMOND [28] with additional crystallographic analysis employing PLATON [29].

Table 1

Summary of the crystallographic data for **1**–**3**.

	1	**2**	**3**
Formula	$C_{20}H_{14}Cl_2N_2OS$	$C_{14}H_{18}Cl_2N_2OS$	$C_{16}H_{22}Cl_2N_2OS$
Formula weight	401.29	333.26	361.31
Crystal size (mm)	0.08 x 0.14 x 0.16	0.08 x 0.18 x 0.28	0.05 x 0.15 x 0.18
Crystal system	monoclinic	monoclinic	monoclinic
Space group	$P2_1/c$	$P2_1/c$	$P2_1/n$
a/Å	13.2182(2)	13.33360(10)	18.1370(4)

b/Å	14.3820(4)	23.7506(2)	9.66110(10)
c/Å	39.3125(6)	9.90310(10)	21.3995(3)
α/°	90	90	90
β/°	96.965(2)	91.0180(10)	106.520(2)
γ/°	90	90	90
V/Å^3	7418.3(3)	3135.63(5)	3594.91(11)
Z/Z'	16/4	8/2	8/2
D_c/g cm^{-3}	1.437	1.412	1.335
μ/mm^{-1}	4.294	4.942	4.351
θrange/°	3.3–77.5	3.3–77.3	2.8–77.6
Reflections measured	69016	26241	38181
Independent reflections; R_{int}	21284, 0.050	6594, 0.027	7576, 0.036
Reflections with $I > 2\sigma(I)$	19129	6286	6646
Number of parameters	960	371	447
R, obs. data; all data	0.041, 0.046	0.027, 0.028	0.038, 0.044
a; b in wght scheme	0.051; 7.608	0.040; 1.692	0.053; 2.356
R_w, obs. data; all data	0.108, 0.110	0.070, 0.071	0.097, 0.102
GoF (F^2)	1.05	0.95	1.04
$\Delta\rho_{max, min}$ (e Å^{-3})	0.79, -0.64	0.36, -0.38	0.54, -0.30

2.4. Antioxidant activity

Phosphomolybdate assay

The antioxidant activity of **1**–**3** was evaluated according to the method of Prieto *et al*. [30]. An aliquot of 100 µl of compounds was combined with 1 ml of reagent solution (0.6 M sulphuric acid, 28 mM sodium phosphate, and 4 mM ammonium molybdate) in a screw-capped vial. The vials were closed and incubated in a water bath at 95 °C for 90 min. After the samples had cooled to room temperature, the absorbance of the mixture was measured at 695 nm against a blank. The results expressed as ascorbic acid equivalent antioxidant activity.

Ferric reducing power

The reducing power of the synthesized acythiourea derivatives was determined according to the method of Oyaizu [31]. Samples (2.5 ml) in phosphate buffer (2.5 ml, 0.2 M, pH 6.6) were added to potassium ferricyanide (2.5 ml, 1.0%) and the mixture was incubated at 50 °C for 20 min. Trichloroacetic acid (2.5 ml, 10%) was added, and the mixture was centrifuged at 650 x g for 10 min. The supernatant (5.0 ml) was mixed with ferric chloride (5.0 ml, 0.1%), and then the absorbance was read spectrophotometrically at 700 nm. Based on the absorbency value, the ferric reducing power of compounds was expressed.

DPPH radical scavenging activity

The DPPH radical scavenging activity was analyzed for each compound by following method of Sanchez-Moreno *et al*. [32]. The compounds (100 µl) was added to 3.9 ml of DPPH solution (0.025 g/L) and the reactants were incubated at 25 °C for 30 min. Different concentrations of ferulic acid was used as a positive control and ethanol was used instead of compounds in the blank (control). The decrease in absorbance was measured at 515 nm using a

spectrophotometer. The radical scavenging activity of tested samples was calculated and expressed on percentage basis.

Superoxide radical scavenging activity

The capacity of prepared compounds to scavenge the superoxide anion radical was measured according to the method described by Zhishen *et al*. [33]. The reaction mixture was prepared using 3 x 10^{-6} M riboflavin, 1 x 10^{-2} M methionine, 1 x 10^{-4} M nitrobluetetrozolium chloride and 0.1 mM EDTA in phosphate buffered saline (pH 7.4). For the analysis, 3.0 ml of the reaction mixture was taken with 100 µl of compounds in closed tubes and illuminated for 40 min under fluorescent lamp (18 W). The absorbance was then read at 560 nm against the un-illuminated reaction mixture. Results were expressed as superoxide radical scavenging activity on a percentage basis.

2.5. Cytotoxicity

The cytotoxic potential of acylthiourea compounds was evaluated in the EAC cell line. The EAC cells were obtained from Swiss mice after 15 days of cancer induction. The peritoneal fluid containing EAC cells was collected aseptically using a 5 ml syringe and cultured in Dulbecco's modified Eagle's medium supplemented with 10% heat-inactivated foetal bovine serum, 1% nonessential amino acids, and 1% penicillin (5000 IU/mL)-streptomycin (5000 μL/mL) solution at 37 °C under 5% CO_2 atmosphere. Initially the cells were washed with PBS twice, centrifuged and the cell pellet was collected and re-suspended in DMEM medium and incubated at 37 °C for 2 days in a CO_2 incubator.

Synthesized compounds **1**–**3** were treated with EAC cells for 24 h and the cell viability was checked using MTT assay [34]. After attaining 60% confluency, the cells were trypsinized

and dispersed in 96 well plate with a cell count of 9000 cells per well and incubated for 24 h. Then the compounds were added at different concentration and then again incubated for 24 h. At the end, the medium was discarded, cells are washed with PBS and 20 microliter of MTT reagent was added in each well and incubated for 6 h at 37 ºC in a water bath. Then 150 microliter of acidic isopropanol was added and shaken for 30 min on a plate shaker under dark. The absorbance was measured at 540 nm and the percentage of cell viability was calculated and from that the cytotoxicity was derived.

3. Data, value and validation

3.1. Synthesis

Compounds **1**–**3** were synthesized from 2,4-dichlorobenzoyl chloride, potassium thiocyanate and the corresponding secondary amine in dry acetone (Scheme 1). The compound **1** is orange while remaining compounds (**2** and **3)** are white. The synthesized compounds are air-stable and non-hygroscopic in nature, soluble in organic solvents such as *n*-hexane, ethyl acetate, acetone, acetonitrile, benzene, dichloromethane, chloroform, DMSO and DMF, and insoluble in water. The analytical data obtained are in good agreement with the proposed molecular formulae.

3.2. Spectroscopy

The synthesized acylthiourea compound **2** showed two bands at 207 and 286 nm in its UV-vis spectrum, which are ascribed to π–π* and n–π* transitions, respectively. The FT–IR spectrum of **2** exhibited very strong absorption band at 3230 cm^{-1} which suggest the presence of N–H group in its structure. The observation of a strong band at 1661 cm^{-1} and a medium intensity at 1210 cm^{-1} in the FT–IR spectrum of **2** confirmed the presence of C=O and C=S groups, respectively [5]. The ^{1}H NMR spectrum showed a singlet at 10.90 ppm, which has been

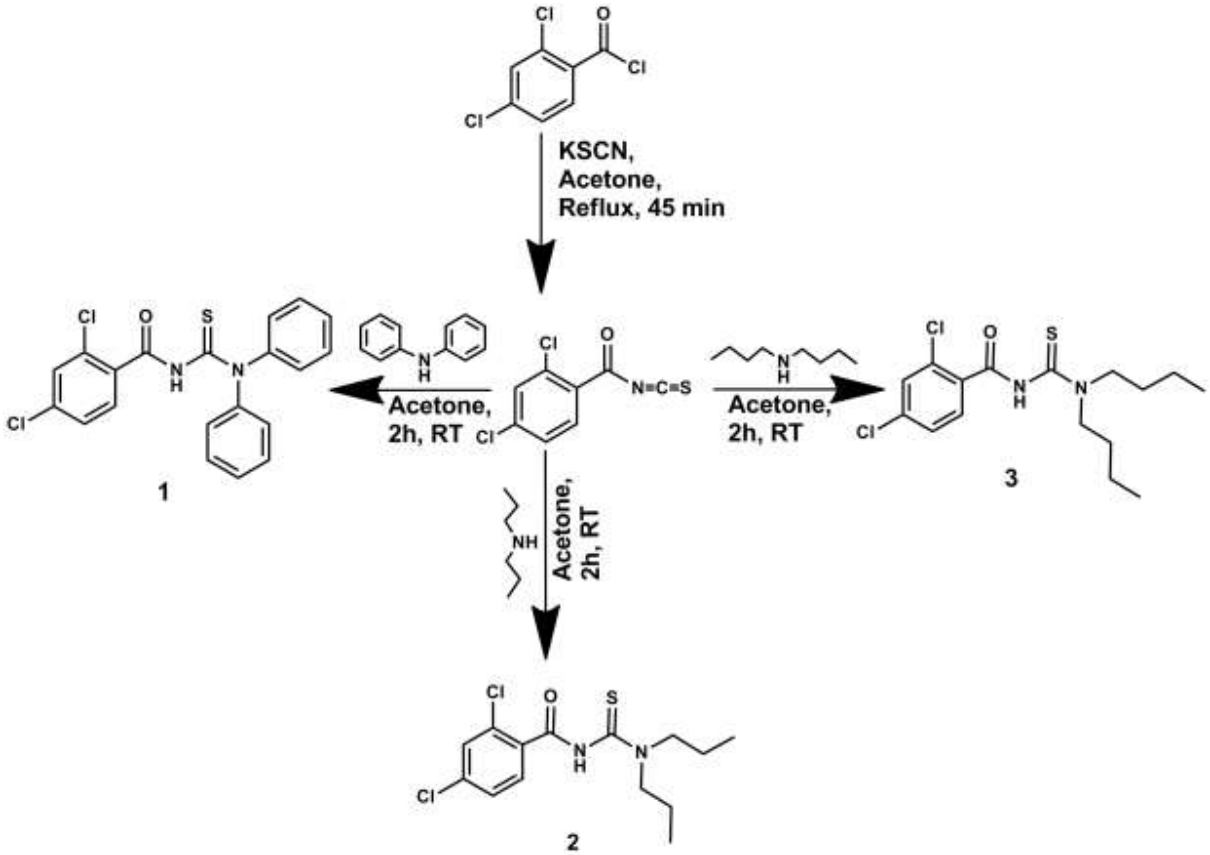

Scheme 1. Synthesis of acyl thiourea compounds.

attributed to the N–H proton of compound **2**. A multiplet observed in the region 7.46–7.69 ppm, in the ^{1}H NMR spectrum of **2**, has been assigned to the aromatic protons of the phenyl ring(s) present in the compound. In addition, ^{1}H NMR spectrum of **2** showed two triplets at 3.85 and 3.54 ppm and a multiplet around 1.65–1.75 ppm, which were assigned to the methylene protons, and two triplets at 0.85 and 0.92 ppm which have been attributed to the terminal methyl protons. The duplication of the resonances is consistent with the non-equivalence of the n-propyl groups in solution. In the ^{13}C NMR spectrum of **2** the signals observed around 128.3–146.4 ppm were assigned to the aryl carbons and signals appeared at 179.8 and 163.2 ppm have been ascribed to C=S and C=O carbons, respectively. The ^{13}C NMR spectrum of **2** exhibited signals related to aliphatic carbons in the expected region.

3.3. X-ray crystallography

The molecular structures of **1**–**3** have been established by single crystal X-ray crystallography, Fig. 1. All three compounds present multiple molecules in their respective crystallographic asymmetric units, i.e. four in **1** (molecules 'a', 'b', 'c' and 'd') and two in each of **2** and **3** (molecules 'a' and b'). Selected geometric parameters for **1**-**3** are collected in Table 2. The thione residue in **1** is flanked on either side by diphenyl amine and amide groups. The C1–N1 bond lengths are systematically longer than the C1–N2 bonds, Table 1. There are also systematic trends in the bond angles subtended at the C1 atom that are related to steric effects. Thus, while the S1–C1–N1 angle is close to 120º, the S1–C1–N2 angle is significantly wider, by about 5º, to relieve steric stress between the doubly bonded sulfur atom and disubstituted amine group, and this is compensated by a smaller angle subtended by the N1 and N2 atoms, Table 2. A similar situation pertains to the angles about the C2 atom with the O1–C1–N1 angles being 8-9º wider than the N1–C2–C3 angles, Table 1. The C1–N1–C2–O1 residues are co-planar with the maximum deviation, i.e. 5.9(5)º, noted for molecule 'd'. However, twists of up to 60º are noted about the C1–N1 bond as manifested in the S1–C1–N1–C2 and N2–C1–N1–C2 torsion angles, and twists in the range 30-40º are seen about the C2–C3 bonds.

The same trends are noted in the C1–N1 vs C1–N2 bond lengths in **2** as for **1** (and **3**). Twists of up 12º are noted about the C1–N2 bond, Table 2, and greater twists are noted in the S1–C1–N1–C2 torsion angles, i.e. 65º. While the N1–C2–C3–C4 torsion angle in **2** are about the same as the equivalent angles in **1**, greater twists, again ca. 65º, are noted in the N2–C1–N1–C2 torsion angles. The substitution of n-propyl groups in **2** for n-butyl in **3** does not have a chemically significant impact upon the molecular geometries, with differences in torsion angles being less than 2º.

Geometric parameters characterizing the molecular packing in **1**–**3** are summarized in Table 3. The most prominent feature of the molecular packing of **1** is the formation of amine-N-H…S(thione) hydrogen bonds between molecules of 'a' and 'd', Fig. 2a, between centrosymmetrically related molecules of 'b', and between centrosymmetrically related molecules of 'c', giving rise to three distinct eight-membered {…HNCS}$_2$ synthons. These are connected into supramolecular layers by C–H…Cl, C–H…O, involving all four independent carbonyl-O atoms, and C–H…S interactions. Layers stack along the c-axis enabling inter-digitation of the chlorophenyl rings. Layers are connected by C–Cl…π(phenyl) and C–S…π(chlorophenyl) interactions to consolidate the three-dimensional crystal, Fig. 2

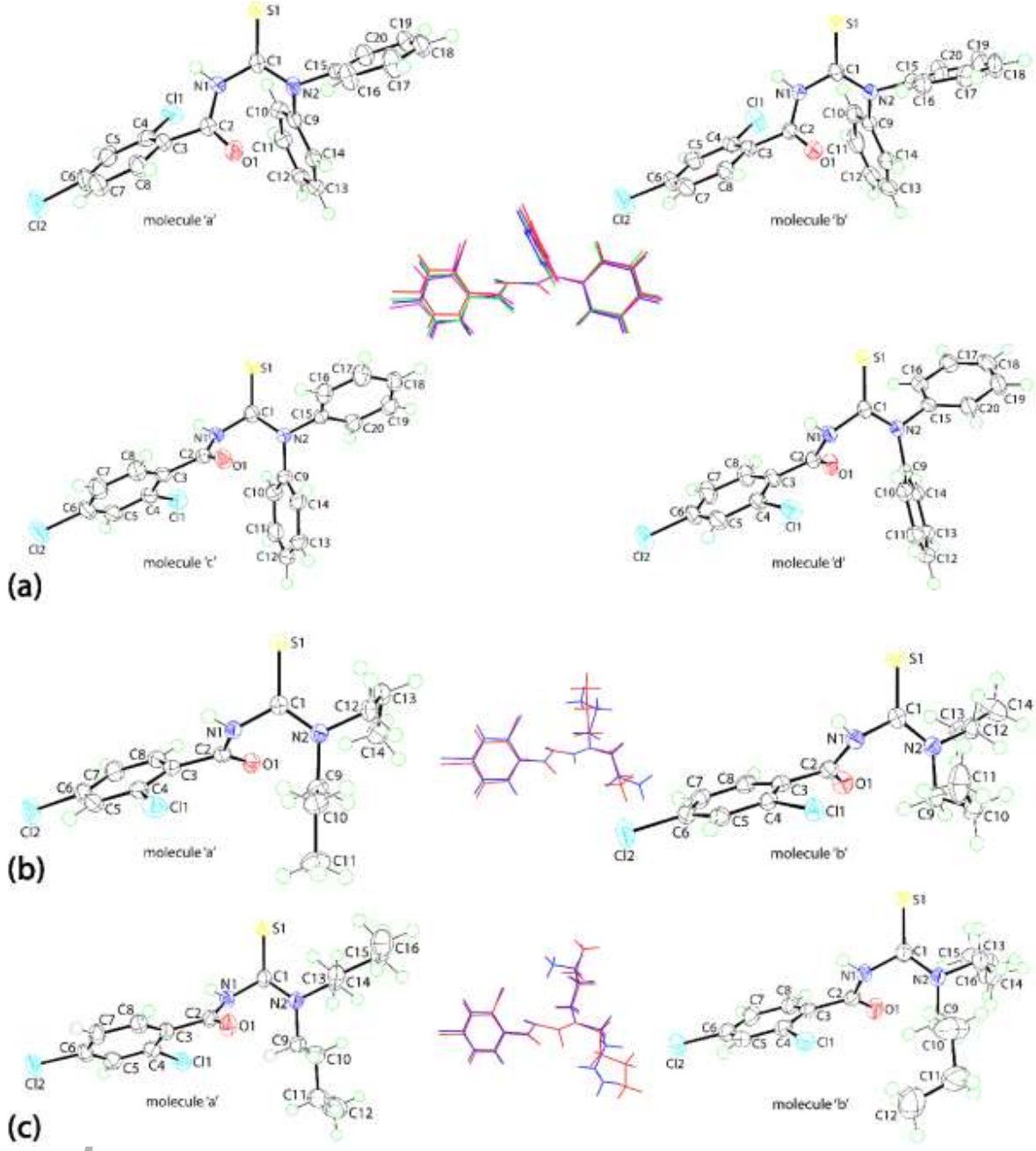

Fig. 1. (a) Molecular structures of the four independent molecules comprising the asymmetric unit of **1**, and overlay diagram showing molecules a (red image), b (green), c (blue) and inverted d (pink), (b) the two independent molecules of **2** and overlay diagrams of molecules a (red image) and b (blue), and (c) the two independent molecules of **3** and overlay diagrams of

molecules a (red image) and inverted b (blue). Only the major component of the disorder is shown in each case. For the overlay diagrams, the molecules have been overlapped so the N_2S atoms are coincident.

In the crystal of **2**, amine-N–H…S(thione) hydrogen bonding between centrosymmetrically related molecules of 'a' leads to the formation eight-membered $\{\ldots HNCS\}_2$ synthons, as for **1**. The second independent molecule associates with the dimer via amide-N–H…O(carbonyl) hydrogen bonding leading to a four molecule aggregate, Fig. 2c, Table 3. These are connected into slabs that stack along the b-axis via C–H…Cl and C–H…π(chlorophenyl) interactions. The most significant inter-layer interactions appear to be halogen bonding. While the Cl2a…Cl2b^{i} separations of 3.5686(6) Å are greater than the sum of the van der Waals radii, i.e. 3.50 Å, the crystal contains chloride-rich channels so that the interactions reinforce each other, Fig. 2d; symmetry operation i: 1-x, 1-y, 1-z.

In **3**, the two independent molecules associate via $\{\ldots HNCS\}_2$ synthons, to form two-molecule aggregates, Table 3. These are connected into supramolecular layers via a combination of C–H…S and C–H…O interactions, Fig. 2e. Connections between layers along the a-axis are again halogen bonding, i.e. Cl1a…Cl1a^{i} = 3.2450(7) Å; symmetry operation i: 1-x,-y,1-z.

Table 2

Selected geometric data (Å, º) for **1**–**3**.

	1a	**1**b	**1**c	**1**d	**2**a	**2**b	**3**a	**3**b
C1–S1	1.667(3)	1.656(3)	1.655(3)	1.662(3)	1.6773(13)	1.6752(13)	1.6812(17)	1.6821(18)
C1–N1	1.393(3)	1.403(3)	1.409(4)	1.404(3)	1.4251(16)	1.4168(16)	1.417(2)	1.419(2)
C1–N2	1.351(4)	1.341(4)	1.354(4)	1.347(4)	1.3242(16)	1.3290(17)	1.325(2)	1.327(2)
C2–O1	1.213(4)	1.218(4)	1.212(4)	1.219(4)	1.2279(16)	1.2204(16)	1.220(2)	1.221(2)
S1–C1–N1	120.0(2)	120.4(2)	120.2(2)	120.0(2)	117.99(9)	117.62(9)	118.29(12)	117.63(12)
S1–C1–N2	123.9(2)	124.6(2)	125.2(2)	123.8(2)	125.47(10)	125.55(10)	125.21(13)	126.22(14)
N1–C1–N2	116.1(3)	115.0(3)	114.6(3)	116.2(2)	116.53(11)	116.83(11)	116.48(15)	116.15(15)
O1–C2–N1	123.7(3)	122.6(3)	123.2(3)	123.0(3)	122.95(11)	123.32(12)	122.95(16)	123.47(16)
O1–C2–C3	121.0(3)	121.3(3)	120.5(3)	120.4(3)	119.84(11)	120.59(12)	120.18(15)	120.39(16)
N1–C2–C3	115.2(2)	116.0(3)	116.2(3)	116.5(2)	117.16(11)	116.08(11)	116.84(14)	116.11(15)
S1–C1–N1–C2	-133.6(3)	-121.3(3)	-125.2(3)	131.5(3)	114.66(11)	115.27(12)	-110.73(16)	112.65(16)
C1–N1–C2–O1	-3.0(5)	0.0(4)	-2.4(5)	5.9(5)	11.54(18)	8.68(19)	-12.9(3)	12.3(3)
N1–C2–C3–C4	49.0(4)	40.3(4)	47.1(4)	-49.5(4)	-46.72(17)	-46.54(17)	46.5(2)	-49.6(2)
N2–C1–N1–C2	48.0(4)	60.9(4)	56.5(4)	-49.0(4)	-65.86(15)	-65.25(16)	68.0(2)	-67.0(2)

Table 3

Summary of intermolecular interactions (Å, º) in **1**–**3**.

	A	H	D	H…D	A…D	A-H…D	Symmetry operation
1							
	N1a	H1a	S1d	2.47(2)	3.331(2)	168(3)	-1+x, y, z
	N1b	H1b	S1b	2.48(3)	3.323(2)	160(2)	-x, 1-y, 1-z
	N1c	H1c	S1c	2.59(3)	3.384(3)	151(3)	1-x, 1-y, -z
	N1d	H1d	S1a	2.52(2)	3.399(2)	173(3)	1+x, y, z
	C8b	H8b	Cl1c	2.79	3.734(3)	172	x, 1½-y, ½+z
	C8c	H8c	Cl1b	2.69	3.565(3)	153	x, ½-y, -½+z
	C11b	H11b	O1c	2.58	3.406(5)	146	x, ½-y, ½+z
	C13a	H13a	O1d	2.51	3.272(3)	137	x, y, z
	C13b	H13b	O1b	2.30	3.159(4)	150	1-x, 1-y, 1-z
	C13c	H13c	O1c	2.58	3.265(4)	130	-x, 1-y, -z
	C13d	H13d	O1a	2.56	3.361(4)	142	x, y, z
	C19a	H19a	S1b	2.84	3.778(4)	171	-x, -½+y, ½-z
	C6b	Cl2b	Cg(C9a-C14a)	3.5380(14)	5.082(3)	147.13(10)	x, ½-y, ½+z
	C1b	S1b	Cg(C3b-C8b)	3.6972(13)	5.235(3)	153.83(11)	-x, 1-y, 1-z
	C1c	S1c	Cg(C3c-C8c)	3.6912(14)	5.262(3)	158.08(11)	1-x, 1-y, -z

2							
	N1a	H1a	S1a	2.652(15)	3.5121(11)	170.2(13)	1-x, 1-y, 2-z
	N1b	H1b	O1a	2.156(15)	3.0216(14)	176.3(13)	x, y, z
	C10b	H10c	Cl1a	2.68	3.5893(15)	152	x, y, -1+z
	C5b	H5b	Cg(C3a-C8a)	2.76	3.4466(13)	129	1-x, 1-y, 1-z
3							
	N1a	H1a	S1b	2.576(10)	3.4542(15)	176(2)	x,-1+y,z
	N1b	H1b	S1a	2.534(11)	3.3939(15)	168(2)	x,1+y,z
	C7a	H7a	S1a	2.87	3.8008(19)	168	x,1+y,z
	C7b	H7b	S1b	2.77	3.709(2)	170	x,-1+y,z
	C13a	H13b	O1a	2.50	3.384(2)	149	½-x,-½+y, ½-z

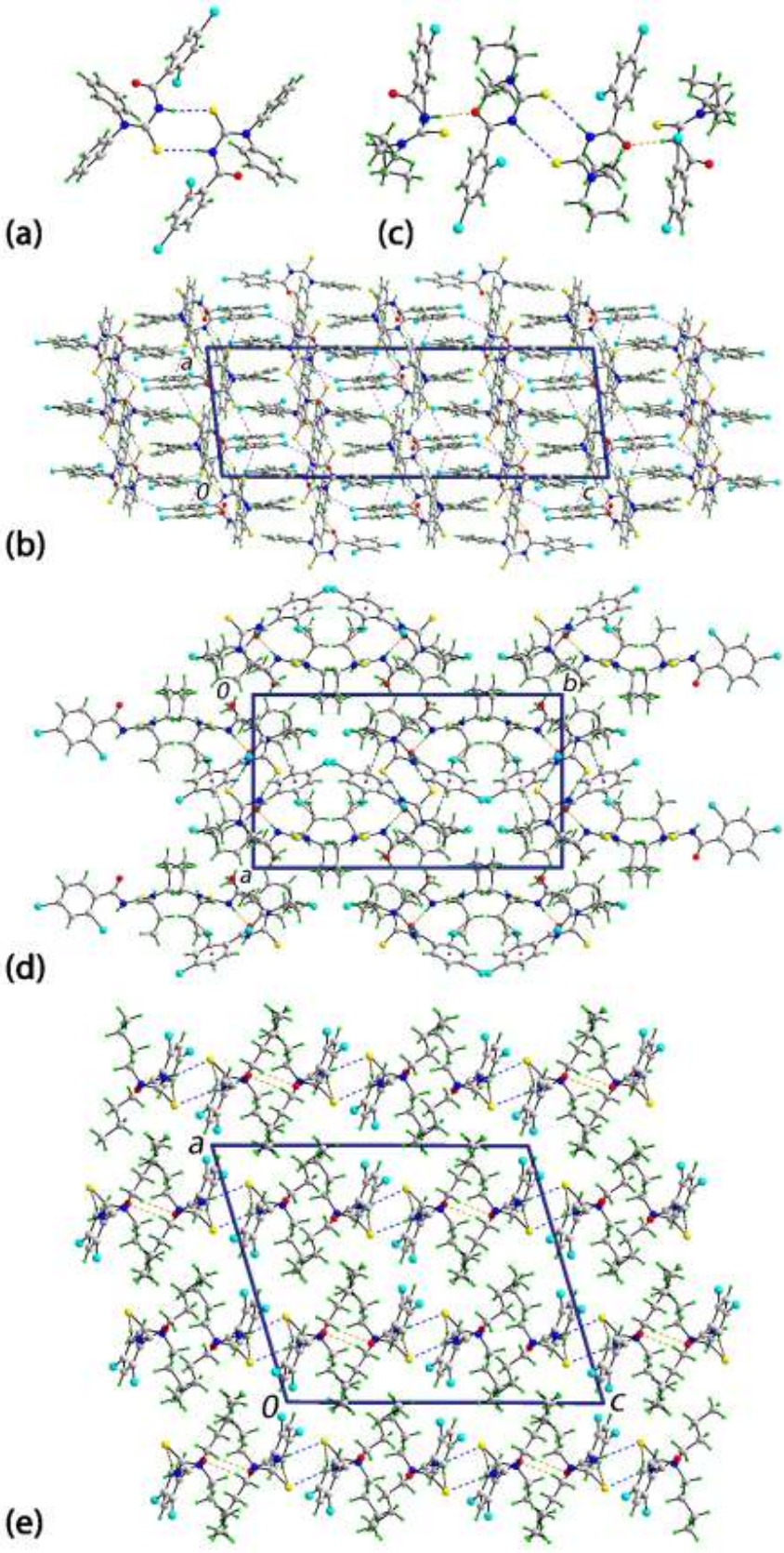
(a)
(c)
a
0
c
(b)
0
b
a
(d)
a
0
c
(e)

Fig. 2. (a) Two molecule aggregate sustained by an eight-membered {…HNCS}$_2$ synthon in **1**, (b) view in projection down the b-axis of the unit cell contents for **1**, (c) four-molecule aggregate in **2** mediated by the {…HNCS}$_2$ synthon and amide-N–H…O(carbonyl) hydrogen bonds, (d) view in projection down the c-axis of the unit cell contents for **2**, and (e) view in projection down the b-axis of the unit cell contents for **3**. The N–H…S hydrogen bonds are shown as blue dashed lines. In (b), the C–H…Cl, O and S interactions are shown as orange dashed lines while the C–Cl…π(phenyl) and C–S…π(chlorophenyl) interactions are shown as pink and purple dashed lines, respectively. In (d) the N–H…O hydrogen bonds and C–H…Cl and C–H…π interactions are shown as orange, brown and purple dashed lines, respectively. In (e) the C–H…O and C–H…S interactions are shown as orange and brown dashed lines, respectively. In (d) and (e) the inter-layer Cl…Cl halogen bonding (see text) is not shown.

3.4. Antioxidant activity

Reactive oxygen species (ROS) are produced in the body as a result of incomplete reduction of oxygen during oxidative phosphorylation [35]. Free radicals can attack DNA and results in mutation and cancer [36]. Free radicals can also react with proteins, carbohydrates and lipids and plays a significant role in the pathogenesis of numerous disorders and patho-physiological processes including cardiovascular diseases, diabetes, and cancer [37]. Oxidative stress occurs, when the system loses its ability to neutralize the excessively produced reactive species. The redox homeostasis, i.e. the balance between the free radicals and antioxidants is necessary for maintaining good health. This balance is maintained by a number of antioxidants (vitamin E and ascorbic acid) and enzymes like catalase, glutathione peroxidise, glutathione-S-transferase, superoxide dismutase, etc. Under severe conditions, above-mentioned antioxidant system is not sufficient to prevent the oxidative stress. Hence, intake of external anti-oxidants is

necessary for maintaining homeostasis in the body. In this connection, several attempts have been made to synthesize molecules and their derivatives with effective antioxidant property in the past [20,21,38]. In the present study also, we have evaluated the antioxidant activity of the three acyl thiourea derivatives, **1**–**3**, as summarized in Fig.3.

In the phosphomolybdate assay, molybdenum(VI) is reduced to molybdenum(V) by an antioxidant to forms a green complex at acidic pH in the presence of phosphorous with an absorption maxima at 695 nm. This assay evaluates the reducing or electron donating power of the antioxidant to molybdenum with the intensity of phosphomolybdate [PMo(V)] complex being proportional to antioxidant power of the extract. The reducing capacity of the trial compound may serve as a significant indicator of its potential antioxidant ability. Among the presently analyzed compounds, **2** recorded a higher level of phosphomolybdate reducing power in dose-dependent manner (96.21%, IC-50 value 29.33 µg/ml), Fig.3a. In the ferric reducing assay, iron(III) is reduced to iron(II) by the antioxidant compound through electron transfer. The reduced iron(II) forms the Pearl's blue complex, which can be measured at 700 nm. Fig. 3b reveals the ferric reducing power of presently investigated compounds and that **2** registered the maximum ferric reducing activity (1.22 absorption units) when compared to the other two compounds (0.63 and 0.96 absorption units).

DPPH (2,2-Diphenyl-1-picrylhydrazyl) is a stable radical, the methanolic solution of which is dark-purple with a maximum absorption at 515 nm. The evaluation of the antioxidant power by DPPH radical scavenging activity has been widely used for different plant extracts and synthetic compounds. Antioxidants can reduce DPPH through hydrogen transfer into its non-radical form (DPPH-H) and hence the absorption disappears at 515 nm. The decrease in absorbency at 515 nm may be due to the reaction between phytochemicals and DPPH, which

indicates the antioxidant power. In the present study, **2** recorded the highest DPPH radical scavenging activity (88.97%, IC-50 value 112.4 µg/ml), which is followed by **3** (83.26%, IC-50 value 161.8 µg/ml) and **1** (70.49%, IC-50 value 372.7 µg/ml), Fig.3c.

Superoxide radical is an oxygen molecule with one unpaired electron. Superoxide is biologically quite toxic and is deployed by the immune system to kill invading microorganisms. In phagocytes, superoxide is produced in large quantities by the enzyme NADPH oxidase for use in oxygen-dependent killing mechanisms of invading pathogens. Although the superoxide anion is a weak oxidant, it gives rise to the generation of powerful and dangerous hydroxyl radicals as well as singlet oxygen, both of which contribute to the oxidative stress. The superoxide radical scavenging activity of samples was investigated by generating superoxide through photo-induced reduction of riboflavin, which can generate superoxide radical in the presence of methionine. The generated superoxide radical reduce the NBT into purple formazan, which was evaluated at 560 nm. In presence of antioxidant, the generated superoxide radicals were scavenged and hence, formation of purple formazan is minimal or nil. The superoxide radical scavenging activity of the synthesized compounds is represented in Fig.3d with compound **2** exhibiting highest activity (93.21%, IC-50 value 148 µg/ml) when compared to compound **3** (80.32%, IC-50 value 229.1 µg/ml), **1** (63.56%, IC-50 value 518.5 µg/ml) and synthetic standard Butylated Hydroxytoluene {BHT} (78.65%, IC-50 value 174.4 µg/ml).

3.5. Cytotoxicity

Cancer is often associated with increased risk of death and the toxic side effects caused by the modern medicine, many cancer patients seek alternative and complementary methods of treatment such as usage of phytomedicine [39]. At present chemotherapy is considered as the most efficient approach for cancer treatment. Even though it significantly improves symptoms

and the quality of life of cancer patients, only modest increases in survival rate can be achieved. As a palliative care, many cancer patients use herbal therapies. Medicinal plants are well known for their free radical scavenging and antioxidant activities [40]. Free radical attack results in the oxidative damage of various biomolecules including lipids, proteins and DNA. The damage caused in DNA leads to mutation or cancer, which is the most dangerous effect in human beings. Plants contain phytochemicals with strong antioxidant activities which may prevent and control cancer and other diseases by protecting the cells from the deleterious effects of the free radicals. In the present time researchers are focusing their research towards the development of eco-friendly anticancer drugs, which resulted in the development of novel chemotherapeutic agents such as paclitaxel, vincristine, podophyllotoxin, and camptothecin.

The newly synthesized acylthiourea derivatives **1**–**3** were screened for their cytotoxic potential against EAC cell lines employing the MTT assay with a view to develop a natural and safe anticancer drug. Among the compounds tested, **2** revealed remarkable level of cytotoxicity (94.7%, IC-50 value 57.25 µg/ml) when compared to **3** (86.44%, IC-50 value 126.3 µg/ml) and **1** (61.53%, IC-50 value 454.8 µg/ml), Fig.4. Cytotoxicity was found to be at a maximum even at very low concentrations, and the death of the cells caused by the test compound might be due to the loss of mitochondria [41]. From the MTT assay, it is evident that the cytotoxicity of the extracts against EAC cell line was dose dependent.

Similar to the present study, Hallur et al. reported the cytotoxicity of benzoylphenylurea sulfur analogues in breast, pancreatic and propstate cancer cell lines [20]. Saeed et al. also evaluated the cytotoxicity of some thiourea derivatives bearing benzothiazole moiety in MCF-7 and Hela cell lines [21]. Further, the cytotoxic effect of nickel(II) complexes synthesized using the 3,3-dialkyl/aryl-1-(2,4-dichlorobenzoyl) thiourea ligands has been

investigated in human lung cancer (A549) and colon cancer cell lines (HT29) [22]. Based on the results obtained from the present study, **2** was found to be more effective in controlling the growth of EAC cell lines when compared to other compounds. Hence, it could be considered as a source of potential anticancer drug and further *in vivo* models must be used to explore the potential of this compound for clinical use.

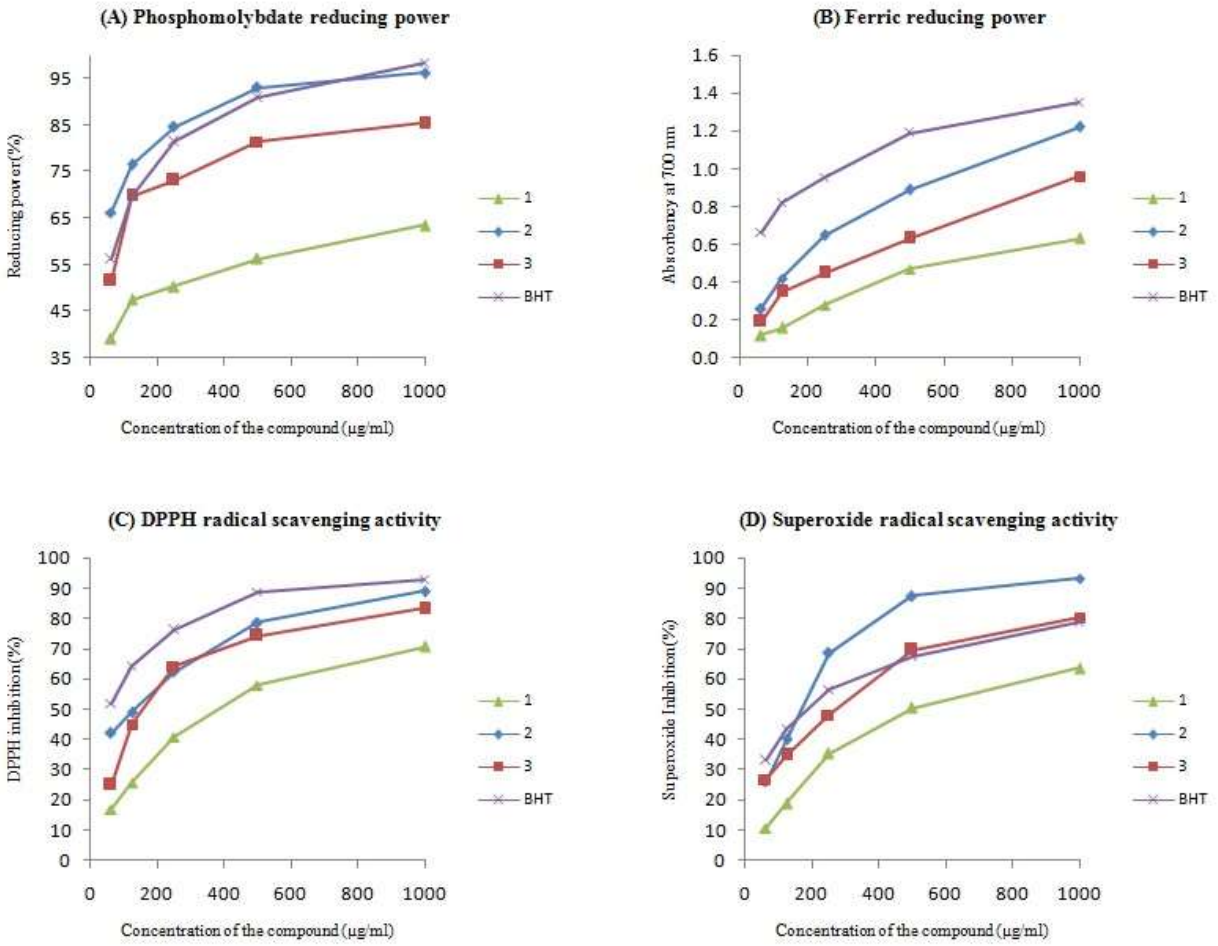

Fig. 3. Antioxidant activity of synthesized compounds: (A) phosphomolybdate reducing power, (B) Ferric reducing power, (C) DPPH radical scavenging activity, and (D) superoxide radical scavenging activity.

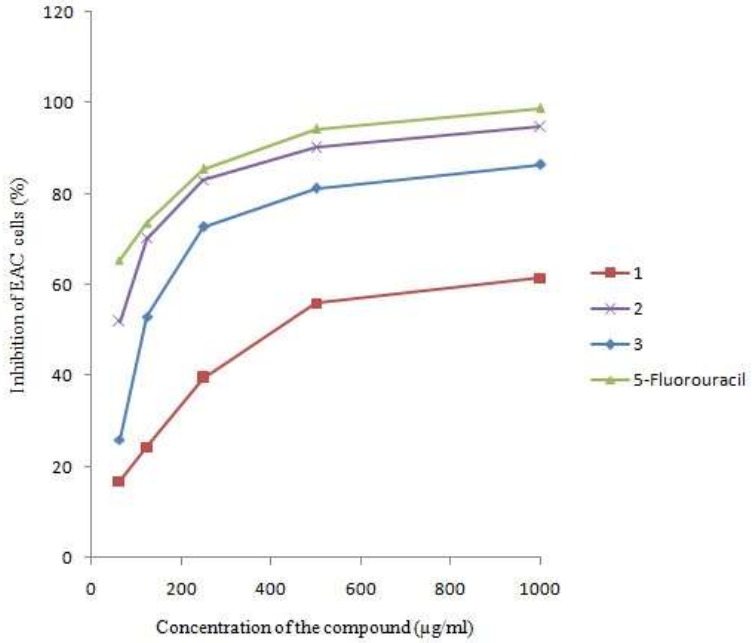

Fig. 4. Cytotoxicity of compounds **1**–**3** against the EAC cancer cell line.

4. Conclusions

In summary, three acylthiourea derivatives, **1**–**3**, were prepared and characterized by analytical and spectral methods. Three dimensional structures of all three compounds were derived by single crystal X-ray crystallography. The acylthiourea derivatives were subjected to *in vitro* antioxidant and cytotoxicity studies. The results indicated that **2** is more effective in exhibiting antioxidant and cytotoxic properties when compared to other compounds. The compound **2** containing two n-propyl carbon chains and **1** is having two aromatic rings on amine nitrogen atom, and hence, the steric effect of the molecules might down-regulate the effect of functional groups. Thus, **1** shows lower antioxidant and cytotoxic properties when compared to other compounds (**2** and **3**). On the other hand, the comparable of antioxidant and cytotoxic activities of compound **3** with those of **2** might be the presence of two n-butyl carbon chains on the amine nitrogen atom of **3**. Hence, based on the preliminary study, the **2** was selected for

further study as it shows promising antioxidant and cytotoxic activities. Further details research is necessary to investigate the cytotoxic potential of this compound in suitable animal model and also to reveal the mechanism of action / pathway through which **2** induces apoptosis and effectively arrest the cell proliferation.

Acknowledgements

N.G. gratefully acknowledges DST, Government of India, for financial assistance under SERB Start-Up Research Grant scheme for Young Scientists (No.SB/FT/CS-189/2013) and SASTRA University for Prof. TRR fund and the infrastructural support.

Appendix A. Supplementary material

CCDC 1493453-1493455 contain the supplementary crystallographic data for this paper. These data can be obtained free of charge from The Cambridge Crystallographic Data Centre via www.ccdc.cam.ac.uk/data_request/cif. Supplementary data associated with this article can be found, in the online version.

References

[1] K.R. Koch, New chemistry with old ligands: N-alkyl- and N,N-dialkyl-N′-acyl(aroyl)thioureas in co-ordination, analytical and process chemistry of the platinum group metals, Coord. Chem. Rev. 216 (2001) 473–488.

[2] M.M. Habtu, S.A. Bourne, K.R. Koch, R.C. Luckay, Competitive bulk liquid membrane transport and solvent extraction of some transition and post-transition metal ions using acylthiourea ligands as ionophores, New J. Chem. 30 (2006) 1155–1162.

[3] N. Gunasekaran, N. Remya, S. Radhakrishnan, R. Karvembu, Ruthenium(II) carbonyl complexes with N-[di(alkyl/aryl)carbamothioyl]benzamide derivatives and triphenylphosphine as effective catalysts for oxidation of alcohols, J. Coord. Chem. 64 (2011) 491–501.

[4] N. Gunasekaran, R. Karvembu, Synthesis, characterization, and catalytic applications of Ru(III) complexes containing N-[di(alkyl/aryl)carbamothioyl]benzamide derivatives and triphenylphosphine/triphenylarsine, Inorg. Chem. Commun. 13 (2010) 952–955.

[5] N. Gunasekaran, P. Ramesh, M.N. Ponnusamy, R. Karvembu, Monodentate coordination of N-[di(phenyl/ethyl)carbamothioyl]benzamide ligands: synthesis, crystal structure and catalytic oxidation property of Cu(I) complexes, Dalton Trans. 40 (2011) 12519–12526.

[6] N. Gunasekaran, P. Jerome, S.W. Ng, E.R.T. Tiekink, R. Karvembu, Tris-chelate complexes of cobalt(III) with N-[di(alkyl/aryl)carbamothioyl]benzamide derivatives: Synthesis, crystallography and catalytic activity in TBHP oxidation of alcohols J. Mol. Catal. A: Chem.353–354 (2012) 156–162.

[7] K. C. Pillai, J. Narayan, Inhibition of corrosion of iron in acids by thiourea and derivatives, J. Electrochem. Soc. 125 (1978) 1393–1397.

[8] M. Ozcan, I. Dehri, M. Erbil, Organic sulphur-containing compounds as corrosion inhibitors for mild steel in acidic media: correlation between inhibition efficiency and chemical structure, Appl. Surf. Sci. 236 (2004) 155–164.

[9] S.S. Abdel-Rehim, K.F. Khaled, N.S. Abd-Elshafi, Electrochemical frequency modulation as a new technique for monitoring corrosion inhibition of iron in acid media by new thiourea derivative, Electrochim. Acta. 51 (2006) 3269–3297.

[10] R.-S. Zeng, J.-P. Zou, S.-J. Zhi, J. Chen, Q. Shen, Novel Synthesis of 1-Aroyl-3-aryl-4-substituted Imidazole-2-thiones, Org. Lett. 5 (2003) 1657–1659.

[11] G.N. Lipunova, E.V. Nosova, A.A. Laeva, T.V. Trashakhova, P.A. Slepukhin, V.N. Charushin, Fluorine-containing heterocycles: XVII. (Tetrafluorobenzoyl)thioureas in the synthesis of fluorine-containing azaheterocycles, Russ. J. Org. Chem. 44 (2008) 741−749.

[12] Z. Zhong, R. Xing, S. Liu, L. Wang, S. Cai, P. Li, Synthesis of acyl thiourea derivatives of chitosan and their antimicrobial activities in vitro, Carbohydr. Res. 343 (2008) 566–570.

[13] A. Saeed, U. Shaheen, A. Hameed, S.Z.H. Naqvi, Synthesis, characterization and antimicrobial activity of some new 1-(fluorobenzoyl)-3-(fluorophenyl)thioureas, J. Fluorine Chem.130 (2009) 1028–1034.

[14] M. Eweis, S.S. Elkholy, M.Z. Elsabee, Antifungal efficacy of chitosan and its thiourea derivatives upon the growth of some sugar-beet pathogens, Int. J. Biol. Macromol. 38 (2006) 1–8.

[15] K. Ramadas, G.Suresh, N. Janarthanan, S. Masilamani, Antifungal activity of 1, 3-disubstituted symmetrical and unsymmetrical thioureas, Pestic. Sci. 52 (1998) 145–151.

[16] X. Xu, X. Qian, Z. Li, Q. Huang, G. Chen, Synthesis and insecticidal activity of new substituted N-aryl-N′-benzoylthiourea compounds, J. Fluorine Chem.121 (2003) 51–54.

[17] X. Sijia, D. Liping, K. Shaoyong, J. Liangbin, Synthesis, crystal structure and herbicidal activity of 1-benzoyl-3-(4,6- disubstitute - pyrimidine-2-yl)-thiourea derivatives, Chem. J. Internet 5 (2003) 67–70.

[18] C. Sun, H. Huang, M. Feng, X. Shi, X. Zhang, P. Zhou, A novel class of potent influenza virus inhibitors: Polysubstituted acylthiourea and its fused heterocycle derivatives, Bioorg. Med. Chem. Lett. 16 (2006) 162–166.

[19] W. Hermindez, E. Spodine, L. Beyer, U. Schrtider, R. Richter, J. Ferreira, M. Pavani, Synthesis, characterization and antitumor activity of copper(II) complexes, [CuL_2] [HL^{1-3}=N,N-Diethyl-N'-(R-benzoyl)thiourea (R=H, o-Cl and p-NO_2)], Bioinorg. Chem. Appl. 3 (2005) 299–316.

[20] G. Hallur, A. Jimeno, S. Dalrymple, T. Zhu, M.K. Jung, M. Hidalgo, J.T. Isaacs, S. Sukumar, E. Hamel, S.R. Khan, Benzoylphenylurea sulfur analogues with potent antitumor activity, J. Med. Chem. 49 (2006) 2357–2360.

[21] S. Saeed, N. Rashid, P.G. Jones, M. Ali, R. Hussain, Synthesis, characterization and biological evaluation of some thiourea derivatives bearing benzothiazole moiety as potential antimicrobial and anticancer agents, Eur. J. Med. Chem. 45 (2010) 1323–1331.

[22] N. Selvakumaran, N.S.P. Bhuvanesh, A. Endo, R. Karvembu, Synthesis, structure, DNA and protein binding studies, and cytotoxic activity of nickel(II) complexes containing 3,3-dialkyl/aryl-1-(2,4-dichlorobenzoyl) thiourea ligands, Polyhedron 75 (2014) 95–109.

[22] Agilent Technologies, CrysAlis PRO. Yarnton, Oxfordshire, England, 2015.

[23] G.M. Sheldrick, A short history of SHELX, ActaCryst. A64 (2008) 112–122.

[24] L.J. Farrugia, WinGX and ORTEP for Windows: an update, J. Appl. Crystallogr. 45 (2012) 849–854.

[25] G.M. Sheldrick, Crystal structure refinement with SHELXL, ActaCryst. C71 (2015) 3–8.

[26] J. Gans, D. Shalloway, Qmol: a program for molecular visualization on Windows-based PCs[1], J. Mol. Graph. Model. 19 (2001) 557–559.

[27] K. Brandenburg, DIAMOND, Crystal Impact GbR, Bonn, Germany, 2006.

[28] A.L. Spek, Single-crystal structure validation with the program PLATON, J. Appl. Crystallogr. 36 (2003) 7–13.

[29] P. Prieto, M. Pineda, M. Aguilar, Spectrophotometric quantitation of antioxidant capacity through the formation of a phosphomolybdenum complex: Specific application to the determination of vitamin E, Anal. Biochem. 269 (1999) 337–341.

[30] M. Oyaizu, Studies on products of browning reactions: Antioxidant activities of products of browning reaction prepared from glucosamine, Jpn. J. Nutr. 44 (1986) 307–315.

[31] C. Sanchez-Moreno, J.A. Larrauri, F.A. Saura-Calixto, A procedure to measure the antiradical efficiency of polyphenols, J. Sci. Food Agr. 76 (1998) 270–276.

[32] J. Zhishen, T. Mengcheng, W. Jianming, The determination of flavonoid contents on mulberry and their scavenging effects on superoxide radical, Food Chem. 64 (1999) 555–559.

[33] T. Mosmann, Rapid colorimetric assay for cellular growth and survival: Application to proliferation and cytotoxicity assays, J. Immunol. Methods 65 (1983) 55–63.

[34] C. Nathan, Specificity of a third kind: Reactive oxygen and nitrogen intermediates in cell signaling, J. Clin. Invest. 111 (2003) 769–778.

[35] M. Perse, Oxidative stress in the pathogenesis of colorectal cancer: Cause or consequence?, Bio. Med. Res. Int. (2013) Article ID 725710.

[36] A. Federico, F. Morgillo, C. Tuccillo, F. Ciardiello, C. Loguercio, Chronic inflammation and oxidative stress in human carcinogenesis, Int. J. Cancer 121 (2007) 2381–2386.

[38] J. Haribabu, G.R. Subhashree, S. Saranya, K. Gomathi, R. Karvembu, D. Gayathri, Synthesis, crystal structure, and *in vitro* and *in silico* molecular docking of novel acyl thiourea derivatives, J. Mol. Struct. 1094 (2015) 281–291.

[39] J. Kim, E.J. Park, Cytotoxic anticancer candidates from natural resources, Cur. Med. Chem. Anticancer Agent 20 (2002) 485–537.

[40] S.K. Agarwal, S. Chatterjee, S.K. Misra, Immune potentiating activity of a poly herbal formulation 'Immu-21', Phytomedica 2 (2001) 1–22.

[41] S.P. Christopher, The significance of spontaneous and induced apoptosis in gastrointestinal tract of mice, Cancer Metstat. Rev. 11 (1992) 179–195.